Electronic Research Archive

ERA, 32(1): 1–16.
DOI: 10.3934/era.2024001
Received: 31 March 2023
Revised: 22 September 2023
Accepted: 21 November 2023
Published: 11 December 2023

http://www.aimspress.com/journal/ERA

Research article

Abnormal dynamics of functional brain network in Apolipoprotein E ε4 carriers with mild cognitive impairment

Xiaoli Yang* and Yan Liu

College of Mathematics and Statistics, Shaanxi Normal University, Xi'an 710119, China

* **Correspondence:** Email: yangxiaoli@snnu.edu.cn.

Abstract: As is well known, the Apolipoprotein E (APOE) ε4 allele is the most pertinent genetic hazardous element for Alzheimer's disease (AD). Mild cognitive impairment (MCI) is considered a prodromal stage of AD. How the APOE ε4 allele modulates functional connectivity of brain network in MCI group is a question worth exploring. At present, some studies have evaluated the relationship between APOE ε4 allele and static functional network connectivity (sFNC) for MCI individuals, while the relationship of dynamic FNC (dFNC) with APOE ε4 allele still remained puzzled. Thus, we aim to detect aberrant dFNC for APOE ε4 carriers in the MCI group. On the basis of the resting-state functional magnetic resonance imaging (rs-fMRI) data, seven intrinsic brain functional networks were first recognized by the group independent component analysis. Then, the technique of sliding window was employed to determine the dFNC, and two dFNC states were detected by the k-means clustering algorithm. Finally, three temporal properties of fraction time, mean dwell time as well as transition numbers in the dFNC states were investigated. The results found that the dFNC and temporal properties in APOE ε4 carriers were abnormal compared with those in APOE ε4 noncarriers. In detail, in the MCI group, compared with APOE ε4 noncarriers, carriers had 9 pairs of abnormal dFNC and had significant differences in all the three temporal properties of the two dFNC states. In addition, two pairs of dFNC were found significantly correlated with clinical measure. This detected abnormal dynamics of temporal properties and dFNC in APOE ε4 carriers were similar with that reported for AD patients in previous studies. These results may suggest that in the MCI group, APOE carriers are more at risk for AD compared to noncarriers. Our findings may offer novel insights into the mechanisms of abnormal brain reconfiguration for individuals at genetic risk for AD, which could also be regarded as biomarkers for the early identification of AD.

Keywords: Apolipoprotein E ε4 carriers; mild cognitive impairment; dynamic functional network

connectivity; rs-fMRI

1. Introduction

Alzheimer's disease (AD) is an irreversible neurological disease, whose primary clinical characteristic is an obvious decline in cognitive function [1]. Mild cognitive impairment (MCI), as the prodromic stage of AD, is a transitional stage between normal aging and early AD [2]. MCI is characterized by performance declines in cognitive domains and is highly likely to develop into AD [3]. Prediction and detection in the stage of MCI can make early prevention, which may postpone the progression to AD. There are a variety of factors that affects the occurrence of AD, involving genetic type, environment and so on [4]. Plaque and tangle production are typical pathological characteristics of AD, which have been the focus on the pathogenesis of AD in recent years [5]. Apolipoprotein E (APOE) genotype is a famous pathogenic factor for AD [6]. More importantly, previous work found that APOE ε4 allele may promote plaque and tangle formation [7]. Note that ε2, ε3 and ε4 are three major APOE alleles, which are with increased risk of AD sequentially giving rise to 6 genotypes (ε2/ε2, ε2/ε3, ε2/ε4, ε3/ε3, ε3/ε4 and ε4/ε4) [8]. Individuals with at least one APOE ε4 allele are called APOE ε4 carriers (including ε2/ε4, ε3/ε4 and ε4/ε4), who have a higher danger and an earlier onset of AD compared with noncarriers [9]. Because of the lack of valid treatments for AD patients, it is important to detect the abnormal brain network in MCI stage so as to diagnose and intervene early.

AD is a multi-network disorder that is not only a localized abnormality in certain areas of the brain but also a large-scale functional brain network abnormality [10]. Large-scale functional network connectivity (FNC) patterns, including inter-network and intra-network connections, were found to be impaired [11]. Previous works have found that AD is related to some abnormal resting-state networks (RSNs) such as the default mode network (DM), cognitive control network (CC), sensorimotor network (SM), visual network (VI) and cerebellum network (CB) [12–16]. Abnormal FNC of RSNs has also been related to cognitive impairment and indicated in neural mechanisms of AD pathophysiology, which could be taken as a possible biomarker of cognitive impairment in AD [17]. Previous studies have found that in the MCI group, APOE ε4 carriers have an enhanced chance of AD compared with noncarriers, i.e., the average age of onset is younger, and cognitive function declines faster [18]. However, the relevant effects of APOE ε4 allele on functional networks for MCI patients have not been fully studied. Identifying gentle changes at network level could be beneficial to reveal the risk of progression to AD for MCI with APOE ε4 carriers at an early stage.

Recent imaging studies on AD spectrum have taken into account the influence of APOE ε4 allele on brain network connectivity [19–23]. Some abnormal static FNC (sFNC), including increased and decreased FNC within the DM in APOE ε4 carriers were revealed. For example, [22,23] have found that APOE ε4 allele can affect FNC in the posterior part of the DM in healthy individuals. However, most previous works about the effect of APOE ε4 allele on brain networks just performed sFNC analysis and focused on normal aging individuals, rather than considering the intrinsic dynamics of neural activity on the whole brain during the MCI phase. Indeed, the human brain connectivity is highly dynamic, and its temporal dynamics can be well captured by dynamic FNC (dFNC) analysis. DFNC analysis can provide elaborate brain connectivity information about functional formation that cannot be detected by sFNC analysis. Inspiringly, based on healthy brains, Sendi et al. have explored the influence of genetic factor on both sFNC and dFNC, finding that genetic risk for AD affected sFNC

wholly and dFNC in women than in men [24]. To our knowledge, there has not been much attention devoted to this topic. Until now, the association between the APOE ε4 allele and dFNC for MCI patients remains largely unclear.

Motivated by the above findings, we focused on the influence of the APOE ε4 allele on the dynamics of functional brain network, examining whether dFNC and the three typical temporal properties are altered in APOE ε4 carriers in MCI group. In this work, we attempted to explore how the dFNC and temporal properties were altered by APOE ε4 allele in the MCI group. For this purpose, the following work was carried out step by step. First, based on the resting-state functional magnetic resonance imaging (rs-fMRI) data of 70 MCI individuals, the techniques of independent component analysis (ICA) and sliding window were implemented to extract the time- dependent functional connectivity networks in the whole brain. Then, the method of k-means algorithm was used to identify the reoccurring dFNC states. Furthermore, the significant differences of temporal properties and dFNC in APOE ε4 carriers were deeply explored compared with noncarriers.

2. Materials and methods

All data in this study were sourced the Alzheimer's Disease Neuroimaging Initiative (ADNI: https://adni.loni.usc.edu/) database. ADNI was initiated in 2003 to explore whether neuropsychological assessments, imaging data, and other biomarkers could be combined so as to prevent and diagnose AD early [25]. Ethical approval has been gotten by the ADNI researchers (http://www.adni-info.org/pdfs/adni_protocol_9_19_08.pdf).

2.1. Participants

A total of 70 MCI subjects (32 APOE ε4 carriers, 38 APOE ε4 noncarriers) were chosen for this study. The diagnosis of subject type (MCI individuals) in ADNI was based on a series of cognitive tests, including Mini-Mental State Examination (MMSE) scores and Clinical Dementia Rating (CDR) scores. Similar with previous studies [1,18], the criteria for choosing the MCI group were that MMSE score was of 24–30 and CDR score was of 0.5, which had mild dementia, but did not meet the diagnostic criteria for AD. The detailed inclusion and exclusion criteria for MCI in the ADNI protocol can be retrieved from http://adni.loni.usc.edu/wp-conte nt/theme s/fresh newa-dev-v2/clini cal/ADNI-1_Proto col.pdf.

2.2. Image acquisition

The image data for the MCI group were obtained by 3-Tesla (3-T) scanners, which were from Philips scanners to ensure the consistency of collection parameters. Structural images were derived by a three-dimensional (3D) MPRAGE T1-weighted sequence. The rs-fMRI data were obtained by an echo-planar sequence with these parameters: Repetition time (TR)/echo time (TE) = 3000/30 ms, slice thickness = 3.3 mm, slice numbers = 48, 140 time points, flip angle = 80. In the course of data collection, all subjects were asked to close eyes rather than fall asleep, relax as much as possible and reduce head movement.

2.3. Data preprocessing

Image data from all participants were pretreated by the Data Processing Assistant for Resting-State fMRI (DPARSF) [26]. First, the first ten time points were abandoned to allow for magnetic field equilibration and subjects adaptation to environments. Then, the rest images were conducted for slice timing and realignment. Subject with excessive head motion (maximum displacement or rotation > 2.0 mm or 2.0° of in any direction) was removed [27]. Next, according to the template of Montreal Neurological Institute, these images were normalized spatially and resampled to cubic voxels with side length of 3 mm, regressing out the nuisance variables (Friston's 24 head motion parameters, global signal, white matter and cerebrospinal fluid signals) [28,29]. Finally, smoothing was performed with a 6-mm full-width at half maximum (FWHM) Gaussian kernel.

2.4. Group Independent Component Analysis (GICA)

Using the Group ICA of fMRI Toolbox (GIFT), group spatial ICA was preformed, and the data were disintegrated into spatial independent components (ICs). A relatively high model order (100 ICs) was used to achieve refined functional segmentation of the brain [30]. Specifically, a two-step principal component analysis (subject-level and group-level) was employed to condense these data [31]. First, the subject-level data were diminished to 120 ICs. Next, the reduced data for all subjects were concatenated into group-level data, which were then further broken down into 100 ICs by the expectation maximization algorithm [32]. We used the infomax ICA algorithm 20 times in ICASSO to ensure the reliability and stability of ICs estimation during the decomposition process [33,34]. At last, we applied the GICA back-reconstruction algorithm to produce subject-level spatial maps and time courses.

According to the criteria of ICs selection in previous works [30,31,35], we further identified meaningful components. Moreover, postprocessing steps of detrending, despiking and filtering with a cutoff frequency of 0.15 Hz were performed for selected ICs [36,37].

2.5. DFNC analysis

The dFNC analysis was conducted based on the technique of sliding window for each subject. We let the window size be 20 TRs (60 s), as it was reported that a window size of 30 to 60 seconds could successfully capture dFNC fluctuations [13]. Next, we convolved these segmented windows were with a Gaussian of $\sigma = 3$ TRs and then slid them in a step length of 1 TR, resulting in 110 successive windows for every participant. Subsequently, the regularized inverse covariance matrix was introduced to eliminate unwanted noise caused by the shorter time series covariance estimation [31]. Specifically, the L1 penalty on the precision matrix was applied to enhance sparsity in the graphic LASSO framework with 100 repetitions [38]. Finally, we z-transformed all the dFNC matrices to ensure stabilizing the variance.

K-means clustering algorithm was conducted on the dFNC matrices for all windows to evaluate the reoccurring dFNC states for all subjects. Owing to the L1 (Manhattan) distance was proved to be an effective method for high dimensional data, it was used to evaluate the intra-cluster similarity between each windowed dFNC matrice and the cluster centroid [31,35]. We repeated the algorithm 100 times in order to decrease the deviation in the initial cluster centroids [35]. The optimal cluster number k was evaluated by the elbow criterion and a state covering at least 10 windows was considered to be reliable.

Here, every cluster denoted a dFNC state [31,35].

For dFNC states, we measured their temporal properties by the following three metrics [27,31,37]: 1) Fraction time, namely, the proportion of total time belonging to each state; 2) mean dwell time, that is, the mean time that each subject was in a given state; 3) transition numbers, i.e., the times that the a state shifted from one to another.

2.6. Statistical analysis

We performed normality test on the age, clinical measure (MMSE scores), temporal properties and dFNC matrices. Then, the differences between APOE ε4 carriers and noncarriers were further checked by two-sample t-test (for normally distributed data) or Mann-Whitney U-test (for non-normally distributed data). We employed χ^2 test to compare the difference of gender between APOE ε4 carriers and noncarriers. For convenience, the Statistical Package for Social Sciences (SPSS 25.0) was performed to the above statistical analyses, with significance thresholds setting at $P < 0.05$, FDR corrected.

2.7. Data availability

In this work, all data were sourced from the ADNI database and are public and freely accessible. Researchers may request and access the data through the ADNI website.

3. Results

3.1. Clinical and demographic measures

One APOE ε4 carrier in the MCI group was excluded due to excessive head motion. Therefore, 69 MCI subjects were kept for further analysis. Table 1 detailed the influence of APOE ε4 allele on demographic and clinical characteristics. These were not significantly different for age and gender between the two subgroups (all $P > 0.05$). Not surprisingly, compared with noncarriers, there was a significant difference in cognitive measure (MMSE scores) for APOE ε4 carriers ($P < 0.05$), which was consistent with the high genetic danger of MCI in APOE ε4 carriers in previous study [9].

Table 1. Demographic and clinical feature of the data.

MCI (n = 69)	ε4+ (n = 31)	ε4- (n = 38)	*P value*
Age	70.97 ± 7.21	74.26 ± 7.59	0.08^a
Sex (M/F)	18/13	17/21	0.9^b
MMSE scores	27.3 ± 1.8	28.32 ± 1.3	0.02^c

Note: ε4+, APOE ε4 carriers; ε4-, APOE ε4 noncarriers. a: two-sample t-test; b: χ^2 test; c: Mann-Whitney U-test.

3.2. GICA components

Based on ICA analysis and empirical selection, 37 ICs were extracted for the MCI group. On the basis of the anatomical and functional characteristics, the ICs were divided into seven networks: Subcortical network (SC), auditory network (AU), SM, VI, DM, CC and CB. As shown in Figure 1(a), the 37 ICs for the MCI group were grouped into the following seven networks: The SC (ICs 22, 30, 40

and 66), the AU (ICs 27, 31 and 41), the SM (ICs 6, 33, 64, 70 and 83), the VI (ICs 7, 28, 35, 36, 37, 52, 74, 76 and 96), the DM (ICs 24, 42, 50, 58, 59 and 72), the CC (ICs 38, 46, 47, 54, 61, 62, 84 and 100) and the CB (ICs 13 and 26).

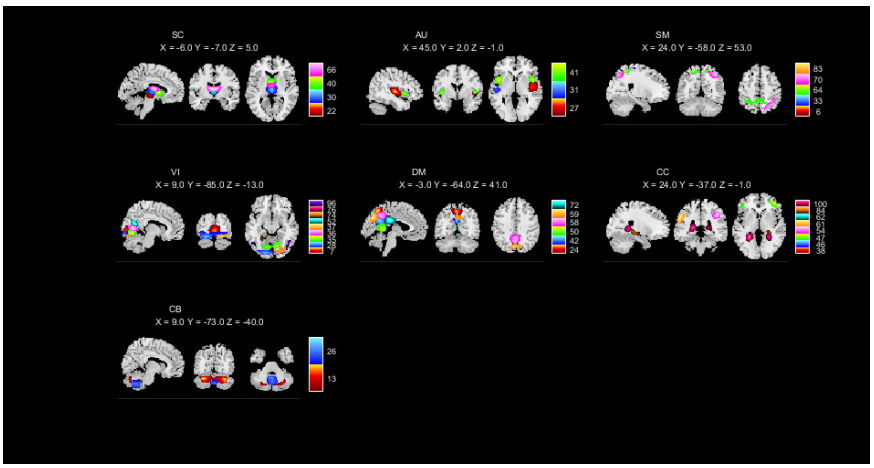

(a)

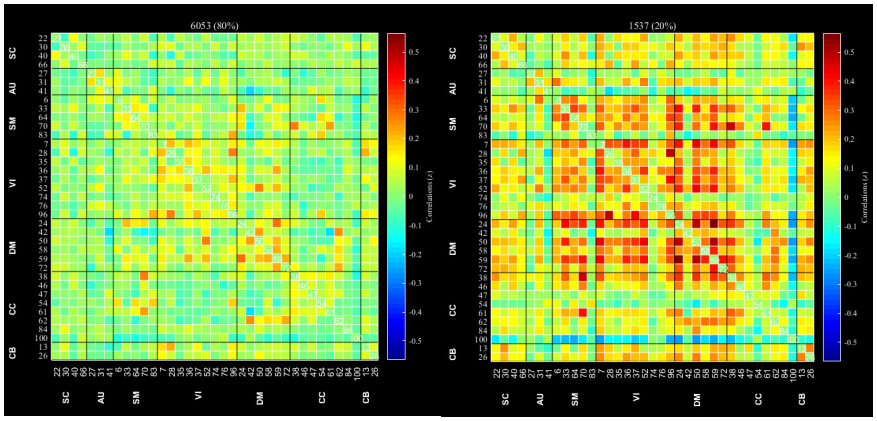

(b)

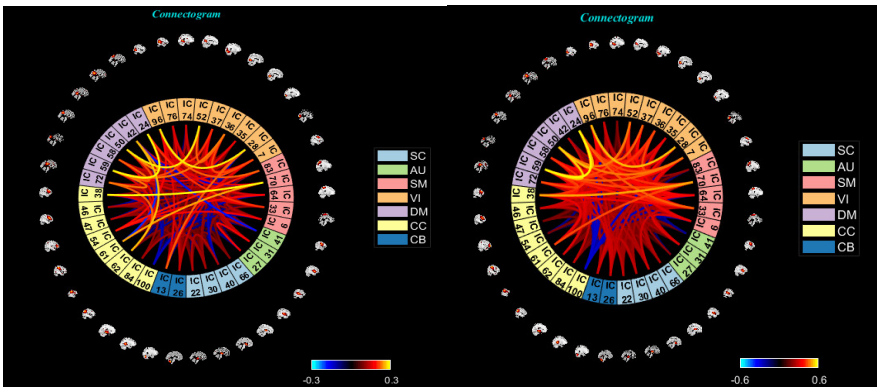

(c)

Figure 1. (a) There were 37 identified meaningful ICs in spatial maps for the MCI group, in which they are divided into 7 functional networks. (b) The two cluster centroids for the two states together with their occurrence rates in the MCI group. The correlation of dFNC between ICs was depicted and demonstrated by a color bar. (c) The dFNC between ICs was described by the connectgrams for the two states. Here, the color bar is ranged from blue (negative) to yellow (positive) gradually.

3.3. DFNC analysis

Using the sliding window method, a number of 37 × 37 connectivity matrices in the 110 windows were obtained for each subject in the MCI group. Every set of symmetric matrices represented the entire dynamic network connectivity for every subject. All dFNC matrices in the MCI group were employed for further k-means clustering analysis. The two dNFC states of the MCI group were determined by k-means clustering analysis. The cluster centroids for the two states and the corresponding occurrence rate were displayed in Figure 1(b). Specifically, for the MCI group, state 1 occurred more frequently (80%) but with relatively weaker connectivity of the whole brain. In comparison, state 2 occurred less frequently (20%) but with partially stronger positive connectivity, mainly within and among the three networks of SM, VI and DM. For better visualization, connectgrams depicting the connections of two dFNC states were displayed in Figure 1(c) for the MCI group.

3.4. Temporal properties of dFNC states

As illustrated in Figure 2, compared to noncarriers, significant differences in temporal properties were observed for APOE ε4 carriers in the MCI group. Compared to noncarriers, both the fraction time and the mean dwell time of APOE ε4 carriers were significantly decreased in state 1 (P = 0.01, P = 0.01, FDR corrected) and enhanced in state 2 (P = 0.009, P = 0.014, FDR corrected). Moreover, APOE ε4 noncarriers had fewer transitions than carriers (P = 0.023, FDR corrected).

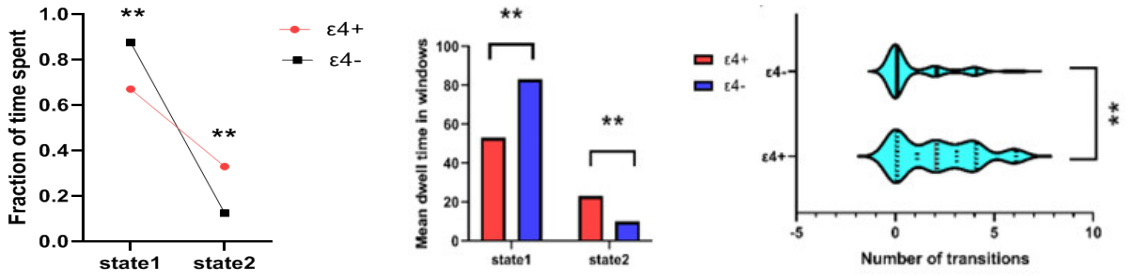

Note: ε4+, APOE ε4 carriers; ε4-, APOE ε4 noncarriers.

Figure 2. Compared to noncarriers, there were differences of the temporal properties for APOE ε4 carriers in the MCI group. ** indicates significant difference under the threshold of P < 0.05.

3.5. DFNC differences

The statistical analysis of two sample t-tests was performed to check if there were significant differences in dFNC between APOE ε4 carriers and noncarriers. Similar with the work [36], we showed only the dFNC with significant differences (P < 0.01) in each state (Table 2). Compared to noncarriers, Figure 3 showed the altered FNC in each state in APOE ε4 carriers in the MCI group.

Table 2. Compared to noncarriers, significant differences of dFNC for APOE ε4 carriers in the MCI group (P < 0.01, FDR corrected).

IC	Network	P value	T value
State 1			
30–35	SC-VI	0.005	-2.89
30–40	SC-SC	0.005	-2.93
26–30	CB-SC	0.003	3.06
36–58	VI-DM	0.007	2.81
58–74	DM-VI	0.009	2.71
State 2			
6–27	SM-AU	0.002	3.51
30–58	SC-DM	0.009	2.82
24–96	DM-VI	0.003	-3.22
24–84	DM-CC	0.006	-2.99

Note: T > 0 indicated increased dFNC in APOE ε4 carriers, while T < 0 indicated decreased dNFC.

Compared to noncarriers, APOE ε4 carriers showed significant dFNC differences in both states. In state 1, APOE ε4 carriers showed abnormal dFNC within SC and SC-CB/VI and VI-DM compared to noncarriers (Figure 3(a)). In state 2, altered dFNC were found in DM-VI/SC/CC and SM-AU in APOE ε4 carriers compared to noncarriers (Figure 3(b)).

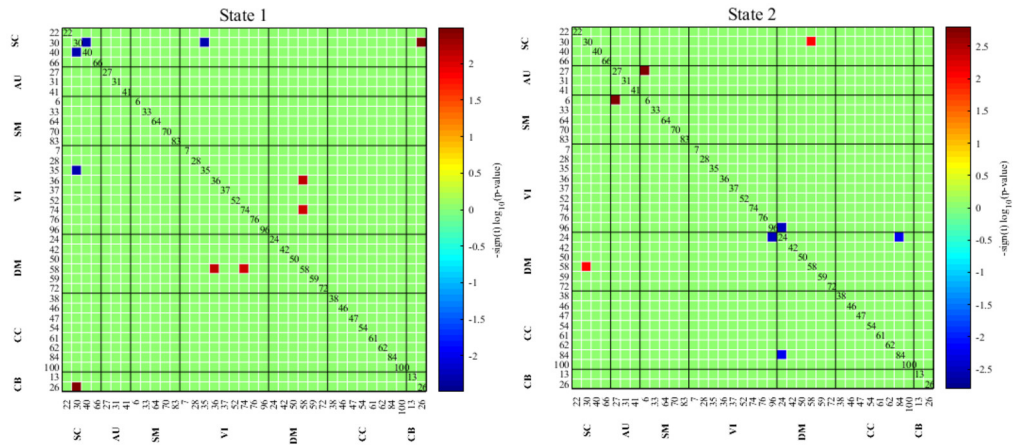

(a) (b)

Figure 3. Compared to noncarriers, abnormal dFNC of APOE ε4 carriers in the MCI group (a) Significantly altered dFNC in state 1 in APOE ε4 carriers compared to noncarriers. (b) Significantly altered dFNC in state 2 in APOE ε4 carriers compared to noncarriers (P < 0.01, FDR corrected). Red/blue squares denoted the brain region where the dFNC was increased/decreased.

Furthermore, correlation analysis was carried out to examine the correlation between abnormal dFNC and MMSE scores. The results revealed that the dFNC between IC 58 (in DM) and IC 74 (in VI) was negatively correlated with MMSE scores significantly (P = 0.044), whereas the dFNC between

IC 24 (in DM) and IC 84 (in CC) was positively correlated with MMSE scores significantly (P = 0.041). These results may imply the dFNC that link precuneus with fusiform gyrus and hippocampus and could help predict the symptom severity in MCI patients (see Figure 4).

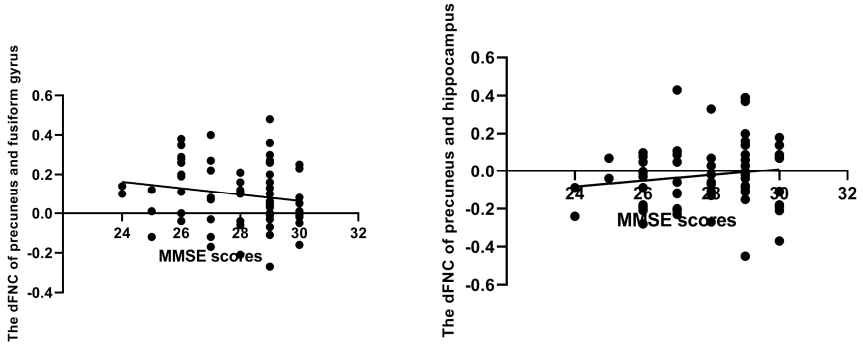

(a) (b)

Figure 4. Significant correlation between abnormal dFNC and MMSE scores.

4. Discussion

Recently, a growing body of research suggests that dFNC may offer novel insights into the pathophysiological mechanisms of some neurodegenerative diseases, such as subjective cognitive decline (SCD), amyotrophic lateral sclerosis, AD and Parkinson's disease [28,29,39]. In this work, we attempted to explore the whole-brain dFNC patterns in APOE ε4 carriers and noncarriers for MCI group by the techniques of ICA, sliding windows, and k-means clustering. The dFNC analysis can better reflect the time-varying features of the brain, which has considered to be a promising approach for studying temporal alteration in the internal brain formation during resting state [34]. The results of this work detected some impaired dFNC and altered temporal properties in APOE ε4 carriers compared to noncarriers in the MCI group, which may serve as early biomarkers of AD.

4.1. DFNC states

As mentioned above, there were two recurrent dFNC states in the MCI group. State 1 occurred more frequently but with relatively weaker connectivity, while the characteristics of state 2 was lower frequency and stronger partial connectivity. The above findings were consistent with previous studies [28–30,39]. In the present study, state 1 can be considered as a baseline state. The higher frequency of this state may imply that the cerebrum has preferences that having more energy reserve rather than more information transmitting [28,39]. The other state occurred less frequently and had strong connectivity in SM, VI and DM networks, which may reflect neuropsychological processes [39,40].

4.2. Temporal properties of dFNC states

Obviously, we found that the temporal properties of APOE ε4 carriers were significantly different from those of noncarriers. Specifically, APOE ε4 noncarriers had more fraction time and mean dwell time in the weak connectivity state (state 1) than APOE ε4 carriers in the MCI group. To some extent, this result agreed with previous studies that aging is the main reason for the longer mean dwell time in

the weak dFNC state [39,41]. On the other hand, we detected that APOE ε4 carriers had more fraction time, mean dwell time and transition numbers in the strong connectivity state than APOE ε4 noncarriers, which may be the result of a compensatory response to degraded dFNC. Notably, the pattern of brain network reorganization in the MCI group of APOE ε4 carriers in this study was similar to that of another study on AD [28]. Thus, these remarkable differences of the three temporal properties in the MCI group indicated that APOE ε4 carriers in the MCI stage could have more severe disease progression and may be at risk for AD.

4.3. DFNC differences

In the MCI group, we detected some abnormal dFNC in APOE ε4 carriers compared to noncarriers in both states, and the abnormal dFNC was primarily in DM, SC and VI. Specifically, there were 9 pairs of abnormal dFNC, 5 of which were between DM and other RSNs. Abnormal connections of the DM with other RSNs have been widely reported in AD spectrum, suggesting that DM is a research hotspot for AD and its high-risk populations [10,42,43]. In this study, the reduced dFNC between the DM and other RSNs may indicate cognitive deficits in APOE ε4 carriers, while the increased dFNC suggested that APOE ε4 carriers may use additional brain subregions to compensate for cognitive impairment. Notably, the decreased dFNC between precuneus and hippocampus was detected in APOE ε4 carriers compared to noncarriers, which accorded with previous finding on APOE ε4 carriers [44]. Furthermore, we observed increased dFNC between the AU and SM in APOE ε4 carriers, which validated the work suggesting that APOE ε4 allele may affect connectivity between the AU and other networks [45]. Moreover, the abnormal dFNC in APOE ε4 carriers was also observed in SC. Interestingly, the reduced dFNC between hypothalamus and caudate was found within SC network of APOE ε4 carriers in this study, which accorded with previous study that decreased connectivity was observed within the SC including the caudate in AD patients [14]. As the CB may modulate cognitive function in early AD, thus the revealed increased connectivity between the CB and SC may be a compensatory mechanism [46]. In addition, the connectivity between the DM and VI was revealed to be increased in APOE ε4 carriers in this work. A previous study has shown that AD group have higher connectivity between these two networks than that in healthy group [47]. As reported in early AD [14], the altered connectivity involving the fusiform gyrus of the VI in our work was related to face recognition and face recognition disorder. The above findings may suggest that APOE ε4 carriers in the MCI group may have a tendency to develop into AD patients.

Overall, our findings suggested that abnormal dFNC in APOE ε4 carriers involved many brain networks, including the cognitive and perceptual networks, as well as the CB and SC, supporting the fact that AD is a multi-network disease to some extent. Notably, in this study the alterations of dFNC in the DM network all involved the precuneus. The precuneus is mostly concerned with behavioral and cognitive functions, whose impaired function maybe an important feature of AD. The precuneus is an area that is more prone to beta-amyloid (Aβ) deposition, which could serve as evidence of excessive Aβ accumulation in AD pathology [48]. Therefore, abnormal connectivity related with the precuneus in APOE ε4 carriers in this study may be used as a neuroimaging biomarker for early AD. Though subcortical region plays a crucial role in triggering AD, most researches on the AD spectrum have focused on abnormal connectivity at the cortical level and only few studies involved the subcortical region [49]. Previous study has revealed that altered connections in AD patients were predominantly between subcortical and cortical regions [50]. Our result found that the abnormal dFNC in APOE ε4 carriers involved the SC network. Note that the subthalamic nucleus is the main structure of the subthalamus, and a previous study has detected neurofibrillary tangles in the subthalamic nucleus with

advanced AD patients [51]. We also found that dFNC abnormalities in the SC network of APOE ε4 carriers occurred primarily in the subthalamus, which may indicate more severe symptoms in the APOE ε4 carriers. Future research should focus more on the subcortical network.

4.4. Limitations and further research

There are some limitations that need to be noted in this current work. First, based on the rs-fMRI data of 70 MCI individuals, our findings suggested the presence of altered dynamic functional connectivity in APOE ε4 carriers at the MCI stage compared with noncarriers; however, further validation studies on larger datasets are urged. Furthermore, we mainly focused on the impact of the APOE ε4 allele on dynamic brain networks at the MCI stage. Since the degree of brain impairment varies at different diagnosing phase of AD, FNC dynamics could also have various features as the disease progresses [28]. Future studies will consider changes of dFNC at other stages of AD development.

5. Conclusions

As stated above, the APOE ε4 allele is a very important pathogenic element for AD. How the APOE ε4 allele regulates the dynamics of functional brain network is largely unexplored. Thus, this work attempted to study the influence of the APOE ε4 allele on the dynamics of whole functional network in the MCI group using dFNC analysis. Based on the rs-fMRI data of 69 MCI subjects, 37 ICs were first extracted for the MCI group by the technique of ICA. Then, these extracted ICs were grouped into 7 networks of SC, AU, SM, VI, DM, CC and CB. Subsequently, two dFNC states were identified for the MCI group by combining the techniques of sliding window and k-means clustering algorithm. For all the temporal properties of the two dFNC states including fraction time, mean dwell time and transition numbers, APOE ε4 carriers in the MCI group showed significant differences compared with APOE ε4 noncarriers. In terms of dFNC, compared with APOE ε4 noncarriers, carriers in the MCI group had 9 pairs of abnormal dFNC involving all the seven networks of SC, AU, SM, VI, DM, CC and CB. In the MCI group, compared to noncarriers the detected abnormal dynamics of temporal properties and dFNC in APOE ε4 carriers were similar with that reported for AD patients in previous studies. The above findings indicated that APOE ε4 carriers in the MCI stage would be at danger of progressing to AD. Our results indicated that dFNC analysis can provide new insights into brain network reorganization in APOE ε4 carriers in the MCI stage, which can facilitate preclinical detection of patients with early AD.

Use of AI tools declaration

The authors declare they have not used Artificial Intelligence (AI) tools in the creation of this article.

Acknowledgments

This work is partially supported by the National Natural Science Foundation of China (Grant Nos. 11972217, 12372062). The data used in this work is from the ADNI database. Therefore, researchers within ADNI have contributed and/or provided data for the design and implementation of ADNI, but have not participated in the analysis or writing of this work.

Conflict of interest

The authors declare that there are no conflicts of interest.

References

1. X. Liu, Q. Zeng, X. Luo, K. Li, H. Hong, S. Wang, et al., Effects of APOE ε2 on the fractional amplitude of low-frequency fluctuation in mild cognitive impairment: a study based on the resting-state functional MRI, *Front. Aging Neurosci.*, **13** (2021), 1–11. https://doi.org/10.3389/fnagi.2021.591347
2. P. Liang, Z. Wang, Y. Yang, X. Jia, K. Li, Functional disconnection and compensation in mild cognitive impairment: evidence from DLPFC connectivity using resting-state fMRI, *PLoS One*, **6** (2011), e22153. https://doi.org/10.1371/journal.pone.0022153
3. A. Chandra, P. E. Valkimadi, G. Pagano, O. Cousins, G. Dervenoulas, M. Politis, Applications of amyloid, tau, and neuroinflammation PET imaging to Alzheimer's disease and mild cognitive impairment, *Hum. Brain Mapp.*, **40** (2019), 5424–5442. https://doi.org/10.1002/hbm.24782
4. C. Reitz, R. Mayeux, Alzheimer disease: epidemiology, diagnostic criteria, risk factors and biomarkers, *Biochem. Pharmacol.*, **88** (2014), 640–651. https://doi.org/10.1016/j.bcp.2013.12.024
5. P. T. Nelson, I. Alafuzoff, E. H. Bigio, C. Bouras, H. Braak, N. J. Cairns, et al., Correlation of Alzheimer disease neuropathologic changes with cognitive status: a review of the literature, *J. Neuropathol. Exp. Neurol.*, **71** (2012), 362–381. https://doi.org/10.1097/NEN.0b013e31825018f7
6. J. Sheffler, J. Moxley, N. Sachs-Ericsson, Stress, race, and APOE: understanding the interplay of risk factors for changes in cognitive functioning, *Aging Mental Health*, **18** (2014), 784–791. https://doi.org/10.1080/13607863.2014.880403
7. J. Raber, Y. Huang, J. W. Ashford, ApoE genotype accounts for the vast majority of AD risk and AD pathology, *Neurobiol. Aging*, **25** (2004), 641–650. https://doi.org/10.1016/j.neurobiolaging.2003.12.023
8. C. C. Liu, T. Kanekiyo, H. Xu, G. Bu, Apolipoprotein E and Alzheimer disease: risk, mechanisms and therapy, *Nat. Rev. Neurol.*, **9** (2013), 184. https://doi.org/10.1038/nrneurol.2013.32
9. T. Li, B. Wang, Y. Gao, X. Wang, T. Yan, J. Xiang, et al., APOE ε4 and cognitive reserve effects on the functional network in the Alzheimer's disease spectrum, *Brain Imaging Behav.*, **15** (2021), 758–771. https://doi.org/10.1007/s11682-020-00283-w
10. B. C. Dickerson, R. A. Sperling, Large-scale functional brain network abnormalities in Alzheimer's disease: insights from functional neuroimaging, *Behav. Neurol.*, **21** (2009), 63–75. https://doi.org/10.3233/BEN-2009-0227
11. P. Wang, B. Zhou, H. Yao, Y. Zhan, Z. Zhang, Y. Cui, et al., Aberrant intra- and inter-network connectivity architectures in Alzheimer's disease and mild cognitive impairment, *Sci. Rep.*, **5** (2015), 14824. https://doi.org/10.1038/srep14824
12. M. A. Binnewijzend, M. M. Schoonheim, E. Sanz-Arigita, A. M. Wink, W. M. van der Flier, N. Tolboom, et al., Resting-state fMRI changes in Alzheimer's disease and mild cognitive impairment, *Neurobiol. Aging*, **33** (2012), 2018–2028. https://doi.org/10.1016/j.neurobiolaging.2011.07.003
13. M. Sendi, E. Zendehrouh, Z. Fu, J. Liu, Y. Du, E. Mormino, et al., Disrupted dynamic functional network connectivity among cognitive control networks in the progression of Alzheimer's disease, *Brain Connect.*, **13** (2023), 334–343. https://doi.org/10.1089/brain.2020.0847

14. M. Sendi, E. Zendehrouh, R. L. Miller, Z. Fu, Y. Du, J. Liu, et al., Alzheimer's disease projection from normal to mild dementia reflected in functional network connectivity: a longitudinal study, *Front. Neural Circuits*, **14** (2020). https://doi.org/10.3389/fncir.2020.593263
15. J. Huang, P. Beach, A. Bozoki, D. C. Zhu, Alzheimer's disease progressively reduces visual functional network connectivity, *J. Alzheimers Dis. Rep.*, **5** (2021), 549–562. https://doi.org/10.3233/ADR-210017
16. F. Tang, D. Zhu, W. Ma, Q. Yao, Q. Li, J. Shi, Differences changes in cerebellar functional connectivity between mild cognitive impairment and Alzheimer's disease: a seed-based approach, *Front. Neurol.*, **12** (2021). https://doi.org/10.3389/fneur.2021.645171
17. Q. Wang, C. He, Z. Wang, Z. Zhang, C. Xie, Dynamic connectivity alteration facilitates cognitive decline in Alzheimer's disease spectrum, *Brain Connect.*, **11** (2021), 213–224. https://doi.org/10.1089/brain.2020.0823
18. G. Sanabria-Diaz, L. Melie-Garcia, B. Draganski, J. F. Demonet, F. Kherif, Apolipoprotein E4 effects on topological brain network organization in mild cognitive impairment, *Sci. Rep.*, **11** (2021), 845. https://doi.org/10.1038/s41598-020-80909-7
19. H. Song, H. Long, X. Zuo, C. Yu, B. Liu, Z. Wang, et al., APOE effects on default mode network in Chinese cognitive normal elderly: relationship with clinical cognitive performance, *PLoS One*, **10** (2015), e0133179. https://doi.org/10.1371/journal.pone.0133179
20. Y. Zhu, L. Gong, C. He, Q. Wang, Q. Ren, C. Xie, Default mode network connectivity moderates the relationship between the APOE genotype and cognition and individualizes identification across the Alzheimer's disease spectrum, *J. Alzheimer's Dis.*, **70** (2019), 843–860. https://doi.org/10.3233/JAD-190254
21. P. A. Chiesa, E. Cavedo, A. Vergallo, S. Lista, M. C. Potier, M. O. Habert, et al., Differential default mode network trajectories in asymptomatic individuals at risk for Alzheimer's disease, *Alzheimer's Dementia*, **15** (2019), 940–950. https://doi.org/10.1016/j.jalz.2019.03.006
22. H. Lu, S. L. Ma, S. W. Wong, C. W. Tam, S. T. Cheng, S. S. Chan, et al., Aberrant interhemispheric functional connectivity within default mode network and its relationships with neurocognitivefeatures in cognitively normal APOE ε4 elderly carriers, *Int. Psychogeriatrics*, **29** (2017), 805–814. https://doi.org/10.1017/S1041610216002477
23. M. M. Machulda, D. T. Jones, P. Vemuri, E. McDade, R. Avula, S. Przybelski, et al., Effect of APOE ε4 status on intrinsic network connectivity in cognitively normal elderly subjects, *Arch. Neurol.*, **68** (2011), 1131–1136. https://doi.org/10.1001/archneurol.2011.108
24. M. S. E. Sendi, E. Zendehrouh, C. A. Ellis, Z. Fu, J. Chen, R. L. Miller, et al., The link between static and dynamic brain functional network connectivity and genetic risk of Alzheimer's disease, *Neuroimage: Clin.*, **37** (2023), 103363. https://doi.org/10.1016/j.nicl.2023.103363
25. S. G. Mueller, M. W. Weiner, L. J. Thal, R. C. Petersen, C. R. Jack, W. Jagust, et al., Ways toward an early diagnosis in Alzheimer's disease: the Alzheimer's Disease Neuroimaging Initiative (ADNI), *Alzheimer's Dementia*, **1** (2005), 55–66. https://doi.org/10.1016/j.jalz.2005.06.003
26. C. G. Yan, Y. F. Zang, DPARSF: a MATLAB toolbox for "pipeline" data analysis of resting-state fMRI, *Front. Syst. Neurosci.*, **4** (2010). https://doi.org/10.3389/fnsys.2010.00013
27. H. Chen, Z. Zou, X. Zhang, J. Shi, N. Huang, Y. Lin, Dynamic changes in functional network connectivity involving amyotrophic lateral sclerosis and its correlation with disease severity, *J. Magn. Reson. Imaging*, **54** (2021), 239–248. https://doi.org/10.1002/jmri.27521
28. Y. Gu, Y. Lin, L. Huang, J. Ma, J. Zhang, Y. Xiao, et al., Abnormal dynamic functional connectivity in Alzheimer's disease, *CNS Neurosci. Ther.*, **26** (2020), 962–971. https://doi.org/10.1111/cns.13387

29. J. Kim, M. Criaud, S. S. Cho, M. Díez-Cirarda, A. Mihaescu, S. Coakeley, et al., Abnormal intrinsic brain functional network dynamics in Parkinson's disease, *Brain*, **140** (2017), 2955–2967. https://doi.org/10.1093/brain/awx233
30. E. A. Allen, E. Damaraju, S. M. Plis, E. B. Erhardt, T. Eichele, V. D. Calhoun, Tracking whole-brain connectivity dynamics in the resting state, *Cereb. Cortex*, **24** (2014), 663–676. https://doi.org/10.1093/cercor/bhs352
31. G. Li, L. Zhou, Z. Chen, N. Luo, M. Niu, Y. Li, et al., Dynamic functional connectivity impairments in idiopathic rapid eye movement sleep behavior disorder, *Parkinsonism Relat. Disord.*, **79** (2020), 11–17. https://doi.org/10.1016/j.parkreldis.2020.08.003
32. S. Roweis, EM algorithms for PCA and SPCA, in *Advances in Neural Information Processing Systems*, **10** (1997), 626–632. Available from: https://proceedings.neurips.cc/paper_files/paper/1997/file/d9731321ef4e063ebbee79298fa36f56-Paper.pdf.
33. A. J. Bell, T. J. Sejnowski, An information-maximization approach to blind separation and blind deconvolution, *Neural Comput.*, **7** (1995), 1129–1159. https://doi.org/10.1162/neco.1995.7.6.1129
34. T. Yin, Z. He, P. Ma, R. Sun, K. Xie, T. Liu, et al., Aberrant functional brain network dynamics in patients with functional constipation, *Hum. Brain Mapp.*, **42** (2021), 5985–5999. https://doi.org/10.1002/hbm.25663
35. Z. Yao, J. Shi, Z. Zhang, W Zheng, T. Hu, Y. Li, et al., Altered dynamic functional connectivity in weakly-connected state in major depressive disorder, *Clin. Neurophysiol.*, **130** (2019), 2096–2104. https://doi.org/10.1016/j.clinph.2019.08.009
36. E. Agoalikum, B. Klugah-Brown, H. Yang, P. Wang, S. Varshney, B. Niu, et al., Differences in disrupted dynamic functional network connectivity among children, adolescents, and adults with attention deficit/hyperactivity disorder: a resting-state fMRI study, *Front. Hum. Neurosci.*, **15** (2021). https://doi.org/10.3389/fnhum.2021.697696
37. X. Ma, X. Wu, Y. Shi, Changes of dynamic functional connectivity associated with maturity in late preterm infants, *Front. Pediatr.*, **8** (2020). https://doi.org/10.3389/fped.2020.00412
38. J. Friedman, T. Hastie, R. Tibshirani, Sparse inverse covariance estimation with the graphical lasso, *Biostatistics*, **9** (2008), 432–441. https://doi.org/10.1093/biostatistics/kxm045
39. Q. Chen, J. Lu, X. Zhang, Y. Sun, W. Chen, X. Li, et al., Alterations in dynamic functional connectivity in individuals with subjective cognitive decline, *Front. Aging Neurosci.*, **13** (2021). https://doi.org/10.3389/fnagi.2021.646017
40. R. P. Viviano, N. Raz, P. Yuan, J. S. Damoiseaux, Associations between dynamic functional connectivity and age, metabolic risk, and cognitive performance, *Neurobiol. Aging*, **59** (2017), 135–143. https://doi.org/10.1016/j.neurobiolaging.2017.08.003
41. L. Tian, Q. Li, C. Wang, J. Yu, Changes in dynamic functional connections with aging, *Neuroimage*, **172** (2018), 31–39. https://doi.org/10.1016/j.neuroimage.2018.01.040
42. K. Mevel, G. Chételat, F. Eustache, B. Desgranges, The default mode network in healthy aging and Alzheimer's disease, *Int. J. Alzheimer's Dis.*, **2011** (2011), 535816. https://doi.org/10.4061/2011/535816
43. Y. Zhan, J. Ma, A. F. Alexander-Bloch, K. Xu, Y. Cui, Q. Feng, et al., Longitudinal study of impaired intra- and inter-network brain connectivity in subjects at high risk for Alzheimer's disease, *J. Alzheimer's Dis.*, **52** (2016), 913–927. https://doi.org/10.3233/JAD-160008
44. Y. I. Sheline, J. C. Morris, A. Z. Snyder, J. L. Price, Z. Yan, G. D'Angelo, et al., APOE4 allele disrupts resting state fMRI connectivity in the absence of amyloid plaques or decreased CSF Aβ42, *J. Neurosci.*, **30** (2010), 17035–17040. https://doi.org/10.1523/JNEUROSCI.3987-10.2010

45. Z. Yao, B. Hu, J. Zheng, W. Zheng, X. Chen, X. Gao, et al., A FDG-PET study of metabolic networks in apolipoprotein E ε4 allele carriers, *PLoS One*, **10** (2015), e0132300. https://doi.org/10.1371/journal.pone.0132300
46. C. Y. Lin, C. H. Chen, S. E. Tom, S. H. Kuo, Cerebellar volume is associated withcognitive decline in mild cognitive impairment: results from ADNI, *Cerebellum*, **19** (2020), 217–225. https://doi.org/10.1007/s12311-019-01099-1
47. M. Zhang, Z. Guan, Y. Zhang, W. Sun, W. Li, J. Hu, et al., Disrupted coupling between salience network segregation and glucose metabolism is associated with cognitive decline in Alzheimer's disease–a simultaneous resting-state FDG-PET/fMRI study, *Neuroimage: Clin.*, **34** (2022), 102977. https://doi.org/10.1016/j.nicl.2022.102977
48. G. Aghakhanyan, A. Vergallo, M. Gennaro, S. Mazzarri, F. Guidoccio, C. Radicchi, et al., The Precuneus–a witness for excessive Aβ gathering in Alzheimer's disease pathology, *Neurodegener. Dis.*, **18** (2019), 302–309. https://doi.org/10.1159/000492945
49. X. Tang, D. Holland, A. M. Dale, L. Younes, M. I. Miller, Shape abnormalities of subcortical and ventricular structures in mild cognitive impairment and Alzheimer's disease: detecting, quantifying, and predicting, *Hum. Brain Mapp.*, **35** (2014), 3701–3725. https://doi.org/10.1002/hbm.22431
50. E. Lella, N. Amoroso, D. Diacono, A. Lombardi, T. Maggipinto, A. Monaco, et al., Communicability characterization of structural DWI subcortical networks in Alzheimer's disease, *Entropy*, **21** (2019), 475. https://doi.org/10.3390/e21050475
51. P. Mattila, T. Togo, D. W. Dickson, The subthalamic nucleus has neurofibrillary tangles in argyrophilic grain disease and advanced Alzheimer's disease, *Neurosci. Lett.*, **320** (2002), 81–85. https://doi.org/10.1016/s0304-3940(02)00006-x

Appendix

Table A1. Details of selected ICs in the MCI group.

ICs	x	y	z
Subcortical Network (SC)			
IC 22 Putamen	0	-19	-7
IC 30 Subthalamus/hypothalamus	0	-16	2
IC 40 Caudate	-3	2	2
IC 66 Thalamus	-9	-10	14
Auditory Network (AU)			
IC 27 Superior temporal gyrus	45	-16	5
IC 31 Superior temporal gyrus	-54	-25	8
IC 41 Middle temporal gyrus	-42	11	-4
Sensorimotor Network (SM)			
IC 6 Postcentral gyrus	57	-7	26
IC 33 Paracentral lobule	3	-25	71
IC 64 Superior parietal lobule	21	-52	62
IC 70 Superior parietal lobule	30	-67	50
IC 83 Precentral gyrus	-48	-10	41

Continued on next page

ICs	x	y	z
Visual Network (VI)			
IC 7 Cuneus	3	-88	-1
IC 28 Middle occipital gyrus	-21	-88	19
IC 35 Lingual gyrus	9	-73	-7
IC 36 Calcarine gyrus	9	-70	5
IC 37 Right middle occipital gyrus	27	-79	-22
IC 52 Calcarine gyrus	12	-61	17
IC 74 Fusiform gyrus	-15	-55	-4
IC 76 Inferior occipital gyrus	54	-52	8
IC 96 Middle temporal gyrus	51	-67	-7
Default Mode Network (DM)			
IC 24 Precuneus	0	-61	53
IC 42 Posterior cingulate cortex	0	-61	29
IC 50 Anterior cingulate cortex	0	-49	5
IC 58 Precuneus	0	-55	41
IC 59 Precuneus	0	-76	35
IC 72 Posterior cingulate cortex	0	-28	26
Cognitive Control Network (CC)			
IC 38 Middle frontal gyrus	48	17	26
IC 46 Middle cingulate cortex	-48	20	20
IC 47 Inferior frontal gyrus	42	50	-1
IC 54 Supplementary motor area	48	-34	47
IC 61 Insula	-60	-34	32
IC 62 Inferior parietal lobule	48	-58	35
IC 84 Hippocampus	18	-28	-10
IC 100 Superior frontal gyrus	-24	-43	5
Cerebellum Network (CB)			
IC 13 Cerebellum	-27	-73	-31
IC 26 Cerebellum	0	-55	-46

Note: IC, independent component; x, y, z, coordinates (mm) of primary peak locations in the Montreal Neurological Institute space.

AIMS Press